Nonstandard neutral weak boson and elastic electron-proton scattering

W-Y. P. Hwang

Department of Physics, National Taiwan University, Taipei, Taiwan 10764, China,
Department of Physics, Carnegie-Mellon University, Pittsburgh, Pennsylvania 15213,
and P-2 Los Alamos National Laboratory, The University of California, Los Alamos, New Mexico 87545

(Received 18 May 1988; revised manuscript received 1 August 1988)

The prospect of using a precision measurement of parity violation in elastic electron-proton scattering in the GeV range to detect manifestations of the nonstandard neutral weak boson Z'^0 is investigated in some detail. The numerical results indicate that, for an assumed Z'^0 mass of about 300 GeV, the deviation of the predicted parity-violating beam and target asymmetries from those given by the standard Glashow-Weinberg-Salam electroweak theory can be in the vicinity of several percent. Thus, confirmation of the standard model to within an accuracy of a couple of percent in such measurement should yield a severe constraint on the possible existence of the nonstandard neutral weak boson.

I. INTRODUCTION

The possible existence of a nonstandard weak boson Z'^0, in addition to the usual γ and Z^0 in the standard Glashow-Salam-Weinberg (GSW) $SU(2)\times U(1)$ theory,[1] has been suggested by recent studies[2] of $E_8\times E_8$ superstring models as well as by attempts in constructing grand unified theories (GUT's). As pointed out in a recent paper,[3] introduction of a nonstandard Z'^0 into the standard GSW theory requires an extension of the standard Higgs mechanism, so that only the photon γ will remain massless upon spontaneous symmetry breaking. Two simple Higgs scenarios were considered: the $2+1$ Higgs scenario in which the standard Higgs mechanism is augmented by an additional Higgs singlet [under $SU(2)_L$] and the $2+2$ Higgs scenario in which two Higgs doublets are assumed. By requiring both that the standard neutral weak currents as given by the GSW theory be reproduced *exactly* and that the Higgs fields transform like members of the 27 representation of E_6, we obtain[4] the neutral-current interaction, in the $2+1$ Higgs scenario,

$$\mathcal{L}_{NC}=\frac{e}{\sin\theta_W\cos\theta_W}Z^0_\mu N_\mu + \frac{e}{\cos\theta_W}\tan\phi_W Z'^0_\mu N'^{(i)}_\mu + A_\mu e J^{em}_\mu \ , \tag{1}$$

where $\sin\theta_W=e/g$, $\tan\phi_W=g''/g'$, and J^{em}_μ and N_μ are, respectively, the electromagnetic current and standard neutral weak current carried by chiral fermions. The nonstandard neutral weak current $N'^{(i)}_\mu$, which couples chiral fermions to the nonstandard neutral weak boson Z'^0, depends only on the assumed transformation property of the standard Higgs doublet under E_6. Here, i ($=a$, b, or c) denotes the three possible forms for the current, which will be specified later in Sec. II A. It was also argued that other Higgs scenarios are less natural and thereby might be of less practical interest.

In this paper we wish to explore the prospect of detecting manifestations of the nonstandard neutral weak boson using a precision measurement of parity violation in elastic electron scattering at an electron beam energy of a few GeV, an experiment which may become feasible when the Continuous Electron Beam Accelerator Facility (CEBAF) comes into operation in the early 1990s. The primary objective of this study is to determine the constraint on the possible existence of Z'^0, provided that the accuracy of the proposed parity-violation measurement can reach the level of a couple of percent. [As explained later in Sec. III, the parity-violating asymmetries at forward angles (say, between 5° and 20°) are small due to the accidental cancellation that makes $1-4\sin^2\theta_W$ close to zero. Thus, it will be a difficult experiment if these asymmetries are to be measured to within the accuracy of a couple of percent.]

The rest of this paper is organized briefly as follows. In Sec. II the basic ingredients of the formulation are briefly outlined. In Sec. III numerical results are presented along with some discussions. A brief summary of the paper is given in Sec. IV.

II. FORMULATION

In the $SU(2)_L\times U(1)\times U(1)$ electroweak theory, the transition amplitude for elastic electron-proton scattering,

$$e(p_e)+p(p)\rightarrow e(p_e')+p(p') \ , \tag{2}$$

is given by[5]

$$\mathcal{T}=-\frac{e^2}{q^2}i\bar{u}_e(p_e')\gamma_\mu u(p_e)\mathcal{J}_\mu + \frac{G}{\sqrt{2}}i\bar{u}_e(p_e')\gamma_\mu(g_V+g_A\gamma_5)u(p_e)\mathcal{N}_\mu + \frac{G'}{\sqrt{2}}i\bar{u}_e(p_e')\gamma_\mu(g_V'+g_A'\gamma_5)u(p_e)\mathcal{N}'_\mu \ , \tag{3}$$

with $q_\mu\equiv(p-p')_\mu$ and

$$\mathcal{J}_\mu\equiv\langle p(p')\,|\,J^{em}_\mu(0)\,|\,p(p)\rangle \ , \tag{4a}$$

 ©1988 The American Physical Society

$$\mathcal{N}_\mu \equiv \langle p(p') \,|\, [N_\mu^{(V)}(0)+N_\mu^{(A)}(0)] \,|\, p(p)\rangle \;, \tag{4b}$$

$$\mathcal{N}'_\mu \equiv \langle p(p') \,|\, [N_\mu'^{(V)}(0)+N_\mu'^{(A)}(0)] \,|\, p(p)\rangle \;. \tag{4c}$$

Here, $e^2/4\pi$ ($\equiv\alpha$) is the fine-structure constant and G is the Fermi coupling constant. The coupling constant G' will be specified later. The three terms in Eq. (2) correspond to the diagrams illustrated in Fig. 1, respectively. Note that J_μ^{em} and N_μ are already given in the GSW theory. To describe how to use Eqs. (2)–(4) in making predictions, we wish to divide our presentation into three subsections: the currents, nucleon form factors, and cross sections.

A. The currents

For the purpose of the present paper, it is convenient to decompose the hadronic currents into the isovector and isoscalar currents as follows:

$$J_\mu^{\text{em}}(x)=I_\mu^{(3)}(x)+\tfrac{1}{2}Y_\mu(x) \;, \tag{5a}$$

$$N_\mu^{(V)}(x)=h_V I_\mu^{(3)}(x)+h'_V Y_\mu(x) \;, \tag{5b}$$

$$N_\mu^{(A)}(x)=h_A I_\mu^{5(3)}(x)+h'_A Y_\mu^5(x) \;. \tag{5c}$$

Here, we need to consider only the space consisting of *up* and *down* quarks (i.e., the nuclear domain) and electrons. Working with this limited subspace, we find

$$g_V=-1+4\sin^2\theta_W, \quad g_A=-1 \;, \tag{6a}$$

$$\begin{gathered} h_V=1-2\sin^2\theta_W, \quad h'_V=-\sin^2\theta_W \;, \\ h_A=1, \quad h'_A=0 \;. \end{gathered} \tag{6b}$$

Here, we note that, because of the relation $g^2/8M_W^2=G/\sqrt{2}$, we need to multiply the quark current by a factor of 2 and the leptonic current by a factor of 4 as we go from the currents defined in Eq. (1) to the currents associated with Eq. (3). (Since there are two interference terms between the quark and lepton sectors, we throw this factor of 2 into "redefined" leptonic currents.)

Working with the same subspace, we have obtained in Ref. 4 the nonstandard neutral weak current which is associated with Eq. (1):

$$N_\mu'^{(a)}=-i\bar{d}_R\gamma_\mu\tfrac{1}{2}d_R-i\,\bar{e}_L\gamma_\mu\tfrac{1}{2}e_L-i\bar{\nu}_L\gamma_\mu\tfrac{1}{2}\nu_L \;, \tag{7a}$$

$$\begin{aligned} N_\mu'^{(b)}=&\tfrac{1}{2}i\bar{u}_L\gamma_\mu\tfrac{1}{2}u_L+\tfrac{1}{2}i\bar{d}_L\gamma_\mu\tfrac{1}{2}d_L \\ &+\tfrac{1}{2}i\bar{u}_R\gamma_\mu\tfrac{1}{2}u_R-\tfrac{1}{2}i\bar{d}_R\gamma_\mu\tfrac{1}{2}d_R \\ &-\tfrac{1}{2}i\,\bar{e}_L\gamma_\mu\tfrac{1}{2}e_L-\tfrac{1}{2}i\bar{\nu}_L\gamma_\mu\tfrac{1}{2}\nu_L+\tfrac{1}{2}i\,\bar{e}_R\gamma_\mu\tfrac{1}{2}e_R \;, \end{aligned} \tag{7b}$$

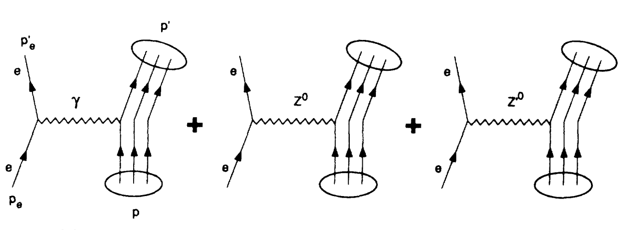

FIG. 1. Elastic electron-proton scattering.

$$\begin{aligned} N_\mu'^{(c)}=&\tfrac{1}{2}i\bar{u}_L\gamma_\mu\tfrac{1}{2}u_L+\tfrac{1}{2}i\bar{d}_L\gamma_\mu\tfrac{1}{2}d_L \\ &+\tfrac{1}{2}i\bar{u}_R\gamma_\mu\tfrac{1}{2}u_R+\tfrac{1}{2}i\,\bar{e}_R\gamma_\mu\tfrac{1}{2}e_R \;, \end{aligned} \tag{7c}$$

depending on whether the Higgs doublet transforms like (a) $(\bar{E},\bar{\nu}'_E)$, (b) (E^{-c},ν_E^c), or (c) (e^{-c},ν_e^c), respectively. [These are the only three colorless $SU(2)_L$ doublets in the 27 representation of E_6.] In addition, we obtain from Eq. (1)

$$\frac{G'}{G}=\tan^2\theta_W\tan^2\phi_W\frac{M_W^2}{M_{Z'}^2} \;, \tag{8}$$

with M_W and $M_{Z'}$ the masses of the charged weak boson and the nonstandard neutral weak boson, respectively. It is amusing to note that, at low energies ($q^2 \ll M_Z'^2$), the two parameters $\tan\phi_W$ and M'_Z associated with the nonstandard weak boson are always correlated together to appear like a single parameter G'/G.

The constraint on the value of G'/G may be obtained from a global fit to the existing data on neutral-current interactions.[6,7] A slightly more stringent constraint has been obtained recently by Marciano and Sirlin[8] by considering box-diagram corrections for charge weak interactions. For the sake of illustration, we adopt $G'/G=\frac{1}{32}$, which corresponds approximately to the most optimistic allowed value for the Z'^0 mass (i.e., about 300 GeV) (Ref. 8). (For the sake of simplicity, we shall simply set $\tan^2\phi_W=1$ since a change in this parameter corresponds *effectively* to a change in the Z'^0 mass.) To describe results for other values of the Z'^0 mass, we shall introduce quantities which describe deviations from the predictions of the standard GSW model and which scale *linearly* with the value of G'/G. [See Eq. (25) below.]

Note that the nonstandard neutral weak current given above may be contrasted with another form used in the literature:[6,7,4]

$$\begin{aligned} N'_\mu=&\tfrac{1}{3}(i\bar{u}_L\gamma_\mu u_L+i\bar{d}_L\gamma_\mu d_L)+\tfrac{1}{3}i\bar{u}_R\gamma_\mu u_R-\tfrac{1}{6}i\bar{d}_R\gamma_\mu d_R \\ &-\tfrac{1}{6}(i\bar{\nu}_L\gamma_\mu\nu_L+i\,\bar{e}_L\gamma_\mu e_L)+\tfrac{1}{3}i\,\bar{e}_R\gamma_\mu e_R \;, \end{aligned} \tag{9}$$

and G' is given by Eq. (8), *but* with $\tan\phi=1$.

We may now decompose the nonstandard neutral weak current into isovector and isoscalar components:

$$N_\mu'^{(V)}(x)=\eta_V I_\mu^{(3)}(x)+\eta'_V Y_\mu(x) \;, \tag{10a}$$

$$N_\mu'^{(A)}(x)=\eta_A I_\mu^{5(3)}(x)+\eta'_A Y_\mu^5(x) \;. \tag{10b}$$

Taking into account appropriate normalization factors in going from Eq. (1) to Eq. (3), we find, for solution (a),

$$\begin{gathered} g'_V=-1, \quad g'_A=-1, \quad \eta_V=\tfrac{1}{2} \;, \\ \eta'_V=-\tfrac{3}{4}, \quad \eta_A=-\tfrac{1}{2}, \quad \eta'_A=\tfrac{3}{4} \;, \end{gathered} \tag{11a}$$

and, for solution (b),

$$\begin{gathered} g'_V=0, \quad g'_A=-1, \quad \eta_V=\tfrac{1}{2} \;, \\ \eta'_V=\tfrac{3}{4}, \quad \eta_A=-\tfrac{1}{2}, \quad \eta'_A=\tfrac{3}{4} \;, \end{gathered} \tag{11b}$$

and, for solution (c),

$$g'_V=\tfrac{1}{2},\quad g'_A=-\tfrac{1}{2},\quad \eta_V=\tfrac{1}{4}\,,$$
$$\eta'_V=\tfrac{9}{8},\quad \eta_A=-\tfrac{1}{4},\quad \eta'_A=\tfrac{3}{8}\,. \tag{11c}$$

As a reference point, we shall consider Eq. (9) as well:

$$g'_V=\tfrac{1}{3},\quad g'_A=-1,\quad \eta_V=\tfrac{1}{2}\,,$$
$$\eta'_V=\tfrac{5}{4},\quad \eta_A=-\tfrac{1}{2},\quad \eta'_A=\tfrac{3}{4}\,. \tag{11d}$$

We wish to use the nonstandard neutral weak currents described above to make predictions on parity violation in elastic electron-proton scattering, focusing mainly on effects caused by Z'^0.

B. Nucleon form factors

We may parametrize the matrix elements of the standard neutral weak current, Eq. (4b), in a Lorentz-covariant manner,

$$\langle p(p')\,|\,N_\mu^{(V)}(0)\,|\,p(p)\rangle \equiv i\bar u_f(p')\left[\gamma_\mu f_V^N(q^2)+\frac{\sigma_{\mu\nu}q_\nu}{2m_p}f_M^N(q^2)-i\frac{q_\mu}{2m_p}f_S^N(q^2)\right]u_i(p)\,, \tag{12a}$$

$$\langle p(p')\,|\,N_\mu^{(A)}(0)\,|\,p(p)\rangle \equiv i\bar u_f(p')\left[\gamma_\mu\gamma_5 f_A^N(q^2)+\frac{\sigma_{\mu\nu}q_\nu\gamma_5}{2m_p}f_E^N(q^2)-i\frac{2m_pq_\mu\gamma_5}{m_\pi^2}f_P^N(q^2)\right]u_i(p)\,, \tag{12b}$$

where $f_V^N(q^2)$, $f_M^N(q^2)$, $f_S^N(q^2)$, $f_A^N(q^2)$, $f_E^N(q^2)$, and $f_P^N(q^2)$ are, respectively, the vector, weak-magnetism, scalar, axial-vector, weak-electricity, and pseudoscalar form factors[9] suitable for the standard neutral weak current. The form factors for the nonstandard neutral weak current can be introduced in an identical fashion and we shall refer to them as $f_j'^N(q^2)$ instead of $f_j^N(q^2)$ (with $j=V, M, S, A, E$, or P).

Analogously, we introduce the nucleon electromagnetic form factors as follows:

$$\langle p(p')\,|\,J_\mu^{\rm em}(0)\,|\,p(p)\rangle \equiv i\bar u_f(p')\left[\gamma_\mu e_p(q^2)+\frac{\sigma_{\mu\nu}q_\nu}{2m_p}\mu_p(q^2)\right]u_i(p)\,, \tag{13a}$$

$$\langle n(p')\,|\,J_\mu^{\rm em}(0)\,|\,n(p)\rangle \equiv i\bar u_f(p')\left[\gamma_\mu e_n(q^2)+\frac{\sigma_{\mu\nu}q_\nu}{2m_p}\mu_n(q^2)\right]u_i(p)\,, \tag{13b}$$

where $e(q^2)$ and $\mu(q^2)$ are the electric charge and anomalous magnetic form factors. Experimentally, one has[10]

$$e_p(q^2=0)=1,\quad \mu_p(q^2=0)=1.793\,, \tag{13c}$$

$$e_n(q^2=0)=0,\quad \mu_n(q^2=0)=-1.913\,, \tag{13d}$$

with the q^2 dependence determined by the standard dipole form with $M_V=0.84$ GeV.

Equations (5a)–(5c) yield, for the standard neutral weak current,

$$f_V^N(q^2)=\tfrac{1}{2}h_V[e_p(q^2)-e_n(q^2)]+h'_V[e_p(q^2)+e_n(q^2)]\,,$$
$$f_M^N(q^2)=\tfrac{1}{2}h_V[\mu_p(q^2)-\mu_n(q^2)]+h'_V[\mu_p(q^2)+\mu_n(q^2)]\,,$$
$$f_S^N(q^2)=0\,, \tag{14a}$$

and, for the nonstandard neutral weak current,

$$f_V'^N(q^2)=\tfrac{1}{2}\eta_V[e_p(q^2)-e_n(q^2)]+\eta'_V[e_p(q^2)+e_n(q^2)]\,,$$
$$f_M'^N(q^2)=\tfrac{1}{2}\eta_V[\mu_p(q^2)-\mu_n(q^2)]+\eta'_V[\mu_p(q^2)+\mu_n(q^2)]\,,$$
$$f_S'^N(q^2)=0\,. \tag{14b}$$

Equations (14a) and (14b) are referred to as the "generalized conserved-vector-current (CVC) theorem"[11] or as the "isotriplet hypothesis."[12] Note that, using $\sin^2\theta_W=0.223$ (Ref. 10), we find

$$f_V^N(q^2=0)=\tfrac{1}{2}(1-4\sin^2\theta_W)=0.054\,,$$

an accidental cancellation as compared to the value of $f_V'^N(0)$ for models (11a)–(11d). This aspect turns out to be of importance when we consider the deviation of the predicted parity-violating asymmetry from that in the GSW theory in the kinematic region of small q_λ.

Analogously, it is customary to define the matrix elements of the charge-lowering weak currents as follows:[9]

$$\langle n(p')\,|\,V_\mu^{(-)}(0)\,|\,p(p)\rangle \equiv i\bar u_f(p')\left[\gamma_\mu f_V(q^2)+\frac{\sigma_{\mu\nu}q_\nu}{2m_p}f_M(q^2)-i\frac{q_\mu}{2m_p}f_S(q^2)\right]u_i(p)\,, \tag{15a}$$

$$\langle n(p')\,|\,A_\mu^{(-)}(0)\,|\,p(p)\rangle \equiv i\bar u_f(p')\left[\gamma_\mu\gamma_5 f_A(q^2)+\frac{\sigma_{\mu\nu}q_\nu\gamma_5}{2m_p}f_E(q^2)-i\frac{2m_pq_\mu\gamma_5}{m_\pi^2}f_P(q^2)\right]u_i(p)\,. \tag{15b}$$

These form factors describe a number of important semileptonic charge weak reactions involving nucleons, including neutron β decay, muon capture in hydrogen, and neutrino-induced muon production on a nucleon target. While the polar-vector form factors $f_V(q^2)$, $f_M(q^2)$, and $f_S(q^2)$ are related to the isovector nucleon electromagnetic form factors via an isospin rotation [conserved vector current (CVC)], the axial-vector form factors $f_A(q^2)$,

$f_E(q^2)$, and $f_P(q^2)$, which have been determined experimentally, provide useful information for neutral weak-interaction studies. Using the "generalized" CVC theorem, we find

$$f_A^N(q^2)=\tfrac{1}{2}h_A f_A(q^2)+h'_A f_A^{(S)}(q^2)\ ,$$

$$f_E^N(q^2)=\tfrac{1}{2}h_A f_E(q^2)+h'_A f_E^{(S)}(q^2)\ , \tag{16a}$$

$$f_P^N(q^2)=\tfrac{1}{2}h_A f_P(q^2)+h'_A f_P^{(S)}(q^2)\ ;$$

$$f_A'^N(q^2)=\tfrac{1}{2}\eta_A f_A(q^2)+\eta'_A f_A^{(S)}(q^2)\ ,$$

$$f_E'^N(q^2)=\tfrac{1}{2}\eta_A f_E(q^2)+\eta'_A f_E^{(S)}(q^2)\ , \tag{16b}$$

$$f_P'^N(q^2)=\tfrac{1}{2}\eta_A f_P(q^2)+\eta'_A f_P^{(S)}(q^2)\ .$$

For studies of the standard neutral weak current, h'_A vanishes identically to lowest order in the GSW theory [Eq. (6b)] and its actual value may be slightly larger than radiative corrections[13] $[O(\alpha)]$, so that it is not essential to know the isoscalar axial-vector form factors $f_A^{(S)}(q^2)$, $f_E^{(S)}(q^2)$, and $f_P^{(S)}(q^2)$. However, the situation for the nonstandard neutral weak current is very different since the value of η'_A as given in Eqs. (11a)–(11d) is as large as the other couplings.

Of course, knowledge of the pseudoscalar form factor is not essential for present studies since it contributes to cross sections with m_e as a proportionality constant. In addition, it is known experimentally that the second-class form factor $f_E(q^2)$ vanishes to a reasonably good approximation, so that it is tempting to assume $f_E^N(q^2)=0$ in making numerical predictions. Experimentally, one has,[10] for the isovector axial-vector form factor,

$$f_A(q^2)=\frac{1.257\pm 0.006}{\left[1+\dfrac{q^2}{M_A^2}\right]^2}\ , \tag{17}$$

with $M_A=1.032\pm 0.036$ GeV (Ref. 14). This leaves the isoscalar axial-vector form factor $f_A^{(S)}(q^2)$ as the only undetermined parameter, which we shall arbitrarily take to be the same as the isovector axial-vector form factor for the sake of illustration. [Note that, in our notation, *only* the products $h'_A f_A^{(S)}(q^2)$ and $\eta'_A f_A^{(S)}(q^2)$ are relevant for cross-section calculations.]

C. Cross sections

In the laboratory frame where the target proton is at rest, we may rewrite Eqs. (12a) and (12b) as follows (with χ_f and χ_i two-component Pauli spinors in the hadron's own rest frame):

$$\mathbf{V}\equiv\langle p(p')\,|\,\mathbf{N}^{(V)}(0)\,|\,p(p)\rangle=\chi_f^\dagger(-i\boldsymbol{\sigma}\times\hat{\mathbf{q}}G_M-\hat{\mathbf{q}}G_s)\chi_i\ , \tag{18a}$$

$$V_0\equiv\langle p(p')\,|\,N_0^{(V)}(0)\,|\,p(p)\rangle=\chi_f^\dagger\chi_i G_V\ , \tag{18b}$$

$$\mathbf{A}\equiv\langle p(p')\,|\,\mathbf{N}^{(A)}(0)\,|\,p(p)\rangle=\chi_f^\dagger(-\boldsymbol{\sigma}G_A-\hat{\mathbf{q}}\,\boldsymbol{\sigma}\cdot\hat{\mathbf{q}}\,G_P)\chi_i\ , \tag{18c}$$

$$A_0\equiv\langle p(p')\,|\,N_0^{(A)}(0)\,|\,p(p)\rangle=\chi_f^\dagger(-\boldsymbol{\sigma}\cdot\hat{\mathbf{q}})\chi_i G_E\ , \tag{18d}$$

with

$$G_M\equiv\xi\{af_M^N(q^2)+b[f_V^N(q^2)-cf_M^N(q^2)]\}\ , \tag{19a}$$

$$G_S\equiv\xi b[f_V^N(q^2)-cf_M^N(q^2)]-\xi af_S^N(q^2)\ , \tag{19b}$$

$$G_V\equiv\xi[f_V^N(q^2)-abf_M^N(q^2)]-\xi cf_S^N(q^2)\ , \tag{19c}$$

$$G_A\equiv\xi[f_A^N(q^2)+cf_E^N(q^2)-abf_E^N(q^2)]\ , \tag{19d}$$

$$G_P\equiv\xi\left[\frac{2m_p\,|\mathbf{q}|}{m_\pi^2}bf_P^N(q^2)+abf_E^N(q^2)\right]\ , \tag{19e}$$

$$G_E\equiv\xi\left[-af_E^N(q^2)-b\left[f_A^N(q^2)-\frac{2m_pq_0}{m_\pi^2}f_P^N(q^2)\right]\right]\ . \tag{19f}$$

Here, we have used

$$\xi\equiv\left[\frac{E_f+m_p}{2E_f}\right]^{1/2}\ , \tag{20a}$$

$$a\equiv\frac{|\mathbf{q}|}{2m_p}\ , \tag{20b}$$

$$b\equiv\frac{|\mathbf{q}|}{E_f+m_p}\ , \tag{20c}$$

$$c\equiv-\frac{q_0}{2m_p}\ . \tag{20d}$$

The differential cross section, as defined in the laboratory frame, for elastic electron-proton scattering is determined by

$$d\sigma=\frac{d^3p'_e}{(2\pi)^3}\frac{d^3p'}{(2\pi)^3}(2\pi)^4\delta^4(p'_e+p'-p_e-p)\overline{\sum}\,|\,\mathcal{T}\,|^2\ , \tag{21}$$

where $\overline{\sum}$ denotes both summation over final discrete states and averaging over initial (unobserved) discrete configurations. Carrying out the summation over final electron spins, we obtain,[15] with $\hat{\mathbf{e}}_i\equiv\mathbf{p}_e/|\mathbf{p}_e|$, $\hat{\mathbf{e}}_f\equiv\mathbf{p}'_e/|\mathbf{p}'_e|$, and $\hat{\mathbf{s}}_e$ the direction of the initial electron polarization,

$$\sum_{s_e'} |\mathcal{T}|^2 = \frac{1}{2}\left[\frac{e^2}{q^2}\right]^2 \{ |\mathbf{J}|^2(1-\hat{\mathbf{e}}_i\cdot\hat{\mathbf{e}}_f)+\mathbf{J}^*\cdot\hat{\mathbf{e}}_f\,\mathbf{J}\cdot\hat{\mathbf{e}}_i+\mathbf{J}\cdot\hat{\mathbf{e}}_f\,\mathbf{J}^*\cdot\hat{\mathbf{e}}_i-2\,\mathrm{Re}[J_0\mathbf{J}^*\cdot(\hat{\mathbf{e}}_i+\hat{\mathbf{e}}_f)]$$
$$+|J_0|^2(1+\hat{\mathbf{e}}_i\cdot\hat{\mathbf{e}}_f)-\hat{\mathbf{s}}_e\cdot\hat{\mathbf{e}}_i\mathrm{Im}[(\hat{\mathbf{e}}_i-\hat{\mathbf{e}}_f)\cdot\mathbf{J}^*\times\mathbf{J}+2J_0\mathbf{J}^*\cdot\hat{\mathbf{e}}_i\times\hat{\mathbf{e}}_f]\}$$
$$+\frac{G}{\sqrt{2}}\left[\frac{e^2}{q^2}\right](g_A\hat{\mathbf{s}}_e\cdot\hat{\mathbf{e}}_i-g_V)\mathrm{Re}[\mathbf{J}^*\cdot\mathbf{N}(1-\hat{\mathbf{e}}_i\cdot\hat{\mathbf{e}}_f)+\mathbf{J}^*\cdot\hat{\mathbf{e}}_f\mathbf{N}\cdot\hat{\mathbf{e}}_i+\mathbf{N}^*\cdot\hat{\mathbf{e}}_f\mathbf{J}\cdot\hat{\mathbf{e}}_i$$
$$-N_0\mathbf{J}^*\cdot(\hat{\mathbf{e}}_i+\hat{\mathbf{e}}_f)-J_0\mathbf{N}^*\cdot(\hat{\mathbf{e}}_i+\hat{\mathbf{e}}_f)+J_0^*N_0(1+\hat{\mathbf{e}}_i\cdot\hat{\mathbf{e}}_f)]$$
$$+\frac{G}{\sqrt{2}}\left[\frac{e^2}{q^2}\right](g_V\hat{\mathbf{s}}_e\cdot\hat{\mathbf{e}}_i-g_A)\mathrm{Im}[(\hat{\mathbf{e}}_i-\hat{\mathbf{e}}_f)\cdot\mathbf{J}^*\times\mathbf{N}+J_0\mathbf{N}^*\cdot\hat{\mathbf{e}}_i\times\hat{\mathbf{e}}_f+N_0\mathbf{J}^*\cdot\hat{\mathbf{e}}_i\times\hat{\mathbf{e}}_f]$$
$$+\frac{G'}{\sqrt{2}}\left[\frac{e^2}{q^2}\right](g_A'\hat{\mathbf{s}}_e\cdot\hat{\mathbf{e}}_i-g_V')\mathrm{Re}[\mathbf{J}^*\cdot\mathbf{N}'(1-\hat{\mathbf{e}}_i\cdot\hat{\mathbf{e}}_f)+\mathbf{J}^*\cdot\hat{\mathbf{e}}_fN'\cdot\hat{\mathbf{e}}_i+\mathbf{N}'^*\cdot\hat{\mathbf{e}}_f\mathbf{J}\cdot\hat{\mathbf{e}}_i$$
$$-N_0'\mathbf{J}^*\cdot(\hat{\mathbf{e}}_i+\hat{\mathbf{e}}_f)-J_0\mathbf{N}'^*\cdot(\hat{\mathbf{e}}_i+\hat{\mathbf{e}}_f)+J_0^*N_0'(1+\hat{\mathbf{e}}_i\cdot\hat{\mathbf{e}}_f)]$$
$$+\frac{G'}{\sqrt{2}}\left[\frac{e^2}{q^2}\right](g_V'\hat{\mathbf{s}}_e\cdot\hat{\mathbf{e}}_i-g_A')\mathrm{Im}[(\hat{\mathbf{e}}_i-\hat{\mathbf{e}}_f)\cdot\mathbf{J}^*\times\mathbf{N}'+J_0\mathbf{N}'^*\cdot\hat{\mathbf{e}}_i\times\hat{\mathbf{e}}_f+N_0'\mathbf{J}^*\cdot\hat{\mathbf{e}}_i\times\hat{\mathbf{e}}_f]\,, \tag{22}$$

where $(\mathbf{J},iJ_0)$ $(\equiv\mathcal{J}_\mu)$, $(\mathbf{N},iN_0)$ $(\equiv\mathcal{N}_\mu)$, and $(\mathbf{N}',iN_0')$ $(\equiv\mathcal{N}_\mu)$ are the matrix elements defined in Eqs. (4a)–(4c).

It is customary to simplify further the expression (22) so that cross sections may be expressed *explicitly* in terms of the various nucleon form factors. (See Ref. 15, as an example.) In this work, we wish to invoke a simple numerical method as an alternative. To this end, we note that, using Eqs. (18)–(20), we may obtain the matrix element $(\mathbf{N},iN_0)$ *numerically* once the nucleon neutral-current form factors are determined from Eqs. (14a), (16a), (13a), (13b), and (17) [with Eqs. (6a) and (6b) as the input]. It is clear that we may obtain in an identical manner the matrix elements $(\mathbf{J},iJ_0)$ and $(\mathbf{N}',iN_0')$. Subsequently, the various vector operations in connection with Eq. (22) can be evaluated *numerically* so that predictions on cross sections can be made on the basis of Eq. (21). In this approach, cross sections for the various spin configurations are evaluated *exactly* in the numerical sense. Although some appealing features associated with analytical expressions of the final formulas may no longer be transparent, the present numerical method *does* offer a straightforward, exact, and viable approach to similar (and more complicated) problems.

Once the cross sections for different spin configurations are obtained, the parity-violating beam asymmetry $\mathcal{A}$ as defined below may be evaluated:

$$\mathcal{A}\equiv\frac{d\sigma(\hat{\mathbf{s}}_e\cdot\hat{\mathbf{e}}_i=+1)-d\sigma(\hat{\mathbf{s}}_e\cdot\hat{\mathbf{e}}_i=-1)}{d\sigma(\hat{\mathbf{s}}_e\cdot\hat{\mathbf{e}}_i=+1)+d\sigma(\hat{\mathbf{s}}_e\cdot\hat{\mathbf{e}}_i=-1)}\,. \tag{23a}$$

Of course, it may also be of interest to consider a parity-violation experiment in which the electrons are not polarized and the target protons are polarized in a certain direction. In this case, we may define the parity-violating target symmetry $\mathcal{B}$:

$$\mathcal{B}\equiv\frac{d\sigma(\hat{\mathbf{s}}_p\cdot\hat{\mathbf{e}}_i=+1)-d\sigma(\hat{\mathbf{s}}_p\cdot\hat{\mathbf{e}}_i=-1)}{d\sigma(\hat{\mathbf{s}}_p\cdot\hat{\mathbf{e}}_i=+1)+d\sigma(\hat{\mathbf{s}}_p\cdot\hat{\mathbf{e}}_i=-1)}\,. \tag{23b}$$

The other quantity which is also of experimental interest is the spin-correlation parameter as defined by

$$\mathcal{C}_{\text{spin}}\equiv\frac{d\sigma(\hat{\mathbf{s}}_e\cdot\hat{\mathbf{s}}_p=+1)-d\sigma(\hat{\mathbf{s}}_e\cdot\hat{\mathbf{s}}_p=-1)}{d\sigma(\hat{\mathbf{s}}_e\cdot\hat{\mathbf{s}}_p=+1)+d\sigma(\hat{\mathbf{s}}_e\cdot\hat{\mathbf{s}}_p=-1)}\,, \tag{24}$$

which, however, is *not* a parity-violating observable. In this paper we shall not consider experiments in which both the beam and the target are not polarized but the polarization of the final proton is detected.

III. NUMERICAL RESULTS AND DISCUSSION

To obtain numerical results, we note that, once the nucleon form factors are known, Eqs. (18)–(20) allow for determination of the various current matrix elements appearing in Eq. (22). Subsequently, Eqs. (21) and (22) yield predictions on cross sections. As mentioned earlier, we choose to carry out these steps *numerically.* As for the input for the nucleon form factors, we assume that $f_A^{(S)}(q^2)=f_A^{(V)}(q^2)$ and that all other form factors are determined through formulas given in Sec. II B. It is clear that, although we do not write out analytical expressions for physical quantities such as those defined in Eqs. (21)–(24), we need not make approximations in generating numerical predictions *once* the nucleon form factors are given.

In Fig. 2(a) we describe the differential cross section $d\sigma/d\Omega_e'$ as a function of the electron scattering angle θ_e for an electron beam energy of 4 GeV (solid curve) and 1 GeV (dashed curve), respectively. Here, the GSW electroweak theory with $\sin^2\theta_W=0.223$ (Ref. 10) (and without the Z'^0) has been used. Note that, at $E_e=4$ GeV and $\theta_e=50°$, the predicted cross section in the GSW theory with both γ and Z^0 is already larger than that of the one-photon exchange *alone* by about 30%. However, it is expected that systematic errors in an experiment will prevent us from using such cross-section measurements to identify the Z^0. Note also that, for $E_e = 4$ GeV, the cross section is already so much forward-peaked that its magnitude at $\theta_e = 5°$ is already smaller than that for $E_e = 1$ GeV.

In Fig. 2(b) we plot the spin-correlation parameter $\mathcal{C}_{\text{spin}}$, as defined by Eq. (24), as a function of the electron scattering angle θ_e for an electron beam energy of 4 and 1 GeV, respectively. Owing to the sizable spin correlation as indicated by this figure, it is clearly of importance to make certain that the beam and the target are not simultaneously polarized in a parity-violation experiment.

In Fig. 2(c) we plot the four-momentum transfer

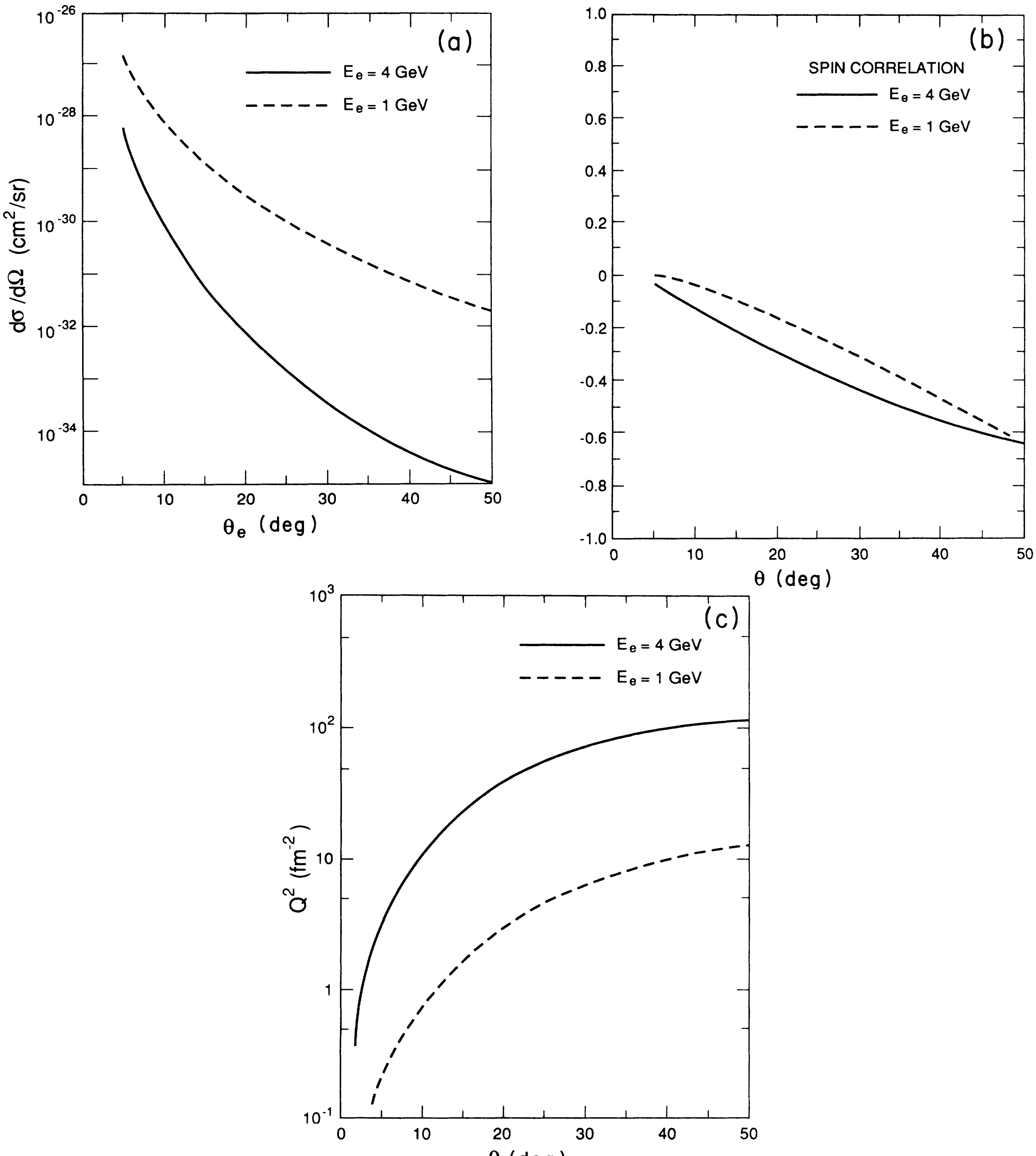

FIG. 2. (a) The differential cross section $d\sigma/d\Omega_e'$ shown as a function of the electron scattering angle θ_e. (b) The spin-correlation parameter $\mathcal{C}_{\text{spin}}$, as defined by Eq. (24), shown as a function of the electron scattering angle θ_e. (c) The four-momentum transfer squared Q^2 shown as a function of the electron scattering angle θ_e.

squared Q^2 ($\equiv q^2$) as a function of the electron scattering angle θ_e for an electron beam energy of 4 and 1 GeV, respectively. Such information is useful since parity-violating asymmetries due to Z^0 or Z'^0 grow approximately linearly with Q^2.

In Fig. 3(a) we describe the beam asymmetry $\mathcal{A}_{\mathrm{GSW}}$, as defined by Eq. (23a) and calculated in the GSW theory with $\sin^2\theta_W = 0.223$, as a function of the electron scattering angle θ_e for an electron beam energy of 4 and 1 GeV, respectively. Note that the magnitude of the beam asymmetry increases approximately linearly with the four-momentum transfer squared Q^2, as reflected by the similarity between Figs. 2(c) and 3(a).

In Fig. 3(b) we describe the target symmetry $\mathcal{B}_{\mathrm{GSW}}$, as defined by Eq. (23b) and calculated in the GSW theory with $\sin^2\theta_W = 0.223$, as a function of the electron scattering angle θ_e for an electron beam energy of 4 and 1 GeV, respectively. Note that the magnitude of the target asymmetry also increases approximately linearly with the four-momentum transfer squared Q^2.

It is useful to observe that, at smaller electron scattering angles (say, less than 10°), the beam asymmetry is dominated quite exclusively by the contribution proportional to the product of the electron axial-vector coupling g_A and the proton polar-vector neutral-current vertex [Eq. (12a)] while the target asymmetry is determined primarily by the contribution proportional to the product of the electron vector coupling g_V and the proton axial-vector neutral-current vertex [Eq. (12b)]. As a numerical example, we note that, at $E_e = 4$ GeV and $\theta_e = 5°$, the predicted beam asymmetry is -2.369×10^{-6} in the GSW electroweak theory with $\sin^2\theta_W = 0.223$, and it remains -2.303×10^{-6} if g_V is set artificially to zero. Meanwhile, the corresponding target asymmetry is 1.681×10^{-6} in the GSW electroweak theory and it becomes 1.478×10^{-6} if g_A is set artificially to zero. At larger electron scattering angles (where cross sections become much smaller), separation between the two contributions becomes considerably less evident.

At forward electron scattering angles (say, between 5° and 20°), we have $q_\lambda \to 0$, so that contributions due to the induced form factors such as $f_M^N(q^2)$ are suppressed. The beam asymmetry in the GSW model is then dictated by $g_A f_V^N(0)$, which is proportional to $1-4\sin^2\theta_W$. Analogously, the target asymmetry is determined primarily by $g_V f_A^N(0)$, which is also proportional to $1-4\sin^2\theta_W$. As a result, the parity-violating asymmetries at forward angles, as exhibited by Figs. 3(a) and 3(b), are small because of the accidental cancellation that makes $1-4\sin^2\theta_W$ close to zero. Thus, it will be a difficult experiment if these asymmetries are to be measured to within the accuracy of a couple of percent. Because of such a cancellation, the "figure of merit" as defined by $\mathcal{A}^2 d\sigma/d\Omega$ becomes a very slow varying function of the electron scattering angle. At $E_e = 4$ GeV, it has a maximum value of 3.69×10^{-10} μb at $\theta_e = 8°$ while, at $E_e = 1$ GeV, it has a maximum value of 2.44×10^{-11} μb at $\theta_e = 33°$. In terms of the calculated figures of merit, an experiment at $\theta_e \approx 20°$ is not much more difficult than that at $\theta_e \approx 10°$ for an electron beam of 4 GeV.

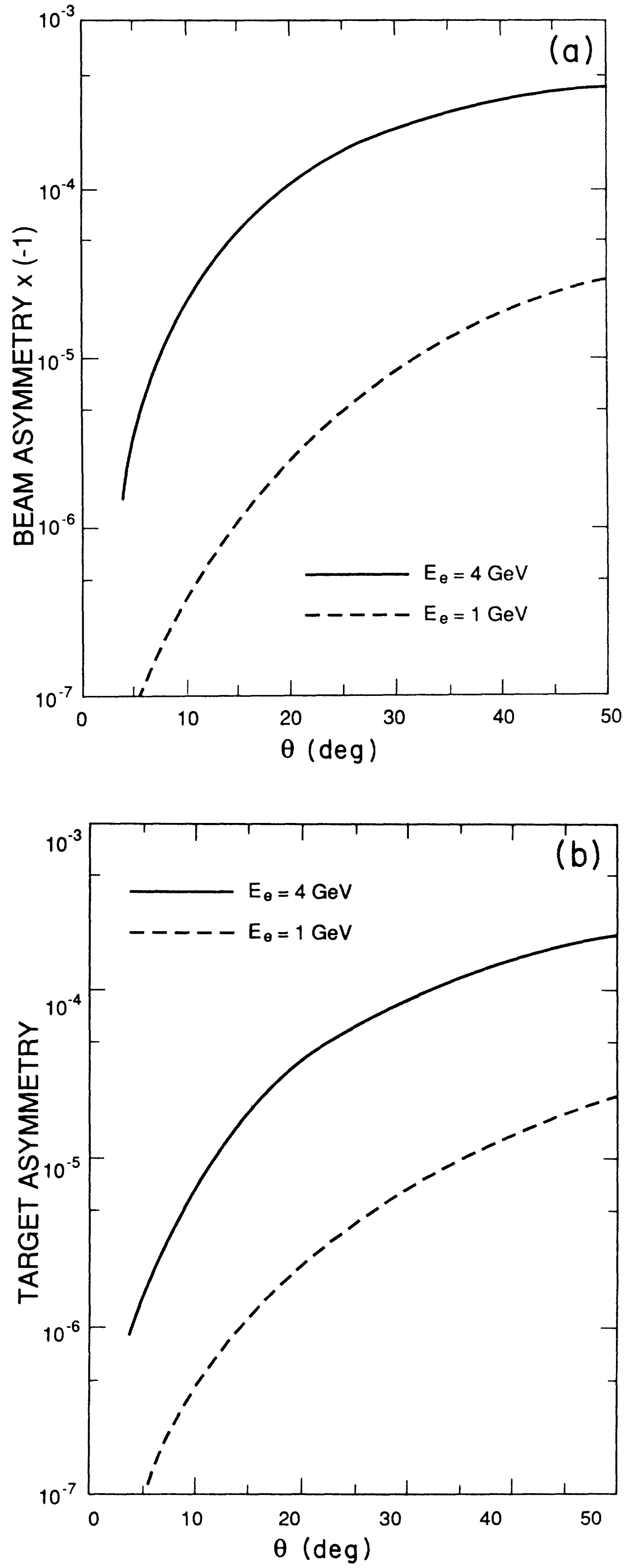

FIG. 3. (a) The beam asymmetry $\mathcal{A}_{\mathrm{GSW}}$, as defined by Eq. (23a) and calculated in the GSW theory with $\sin^2\theta_W = 0.223$, shown as a function of the electron scattering angle θ_e. Note that the asymmetry is predicted to be negative in sign. (b) The target asymmetry $\mathcal{B}_{\mathrm{GSW}}$, as defined by Eq. (23b) and calculated in the GSW theory with $\sin^2\theta_W = 0.223$, shown as a function of the electron scattering angle θ_e.

To contrast different models with the standard GSW theory, it is useful to consider deviations of the predicted asymmetries from the standard-model predictions. To this end, we define

$$\Delta_A \equiv \frac{\mathcal{A} - \mathcal{A}_{\mathrm{GSW}}}{\mathcal{A}_{\mathrm{GSW}}} , \tag{25}$$

where $\mathcal{A}_{\mathrm{GSW}}$ is the asymmetry calculated in the GSW theory (without Z'^0) with $\sin^2\theta_W = 0.223$ (Ref. 10) and $\mathcal{A}$ is the asymmetry calculated in our $SU(2)_L \times U(1) \times U(1)$ electroweak model with the nonstandard neutral weak current specified by Eqs. (11a)–(11d). A definition analogous to Eq. (25) will be adopted for the target asymmetry.

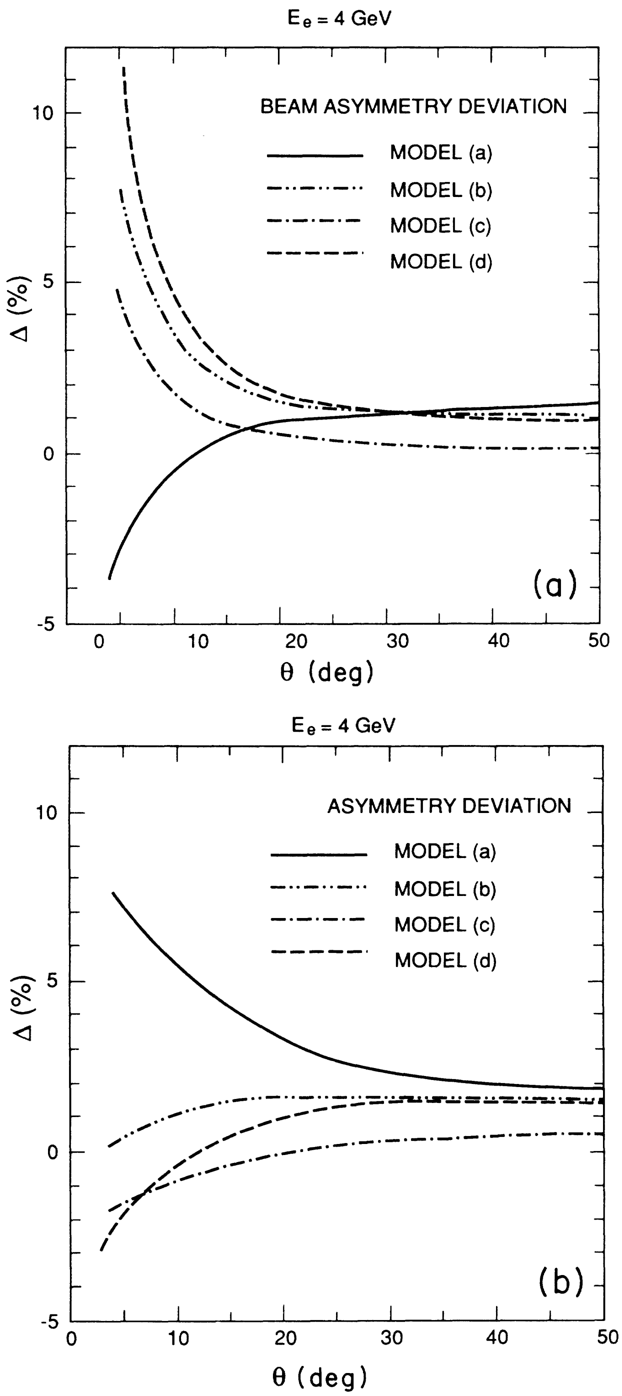

FIG. 4. (a) The quantity Δ, defined by Eq. (25) for the beam asymmetry, shown as a function of the electron scattering angle θ_e at $E_e = 4$ GeV for the four different Z'^0 models of Eqs. (11a)–(11d). (b) The target-asymmetry deviation shown as a function of the electron scattering angle θ_e at $E_e = 4$ GeV for the four different Z'^0 models of Eqs. (11a)–(11d).

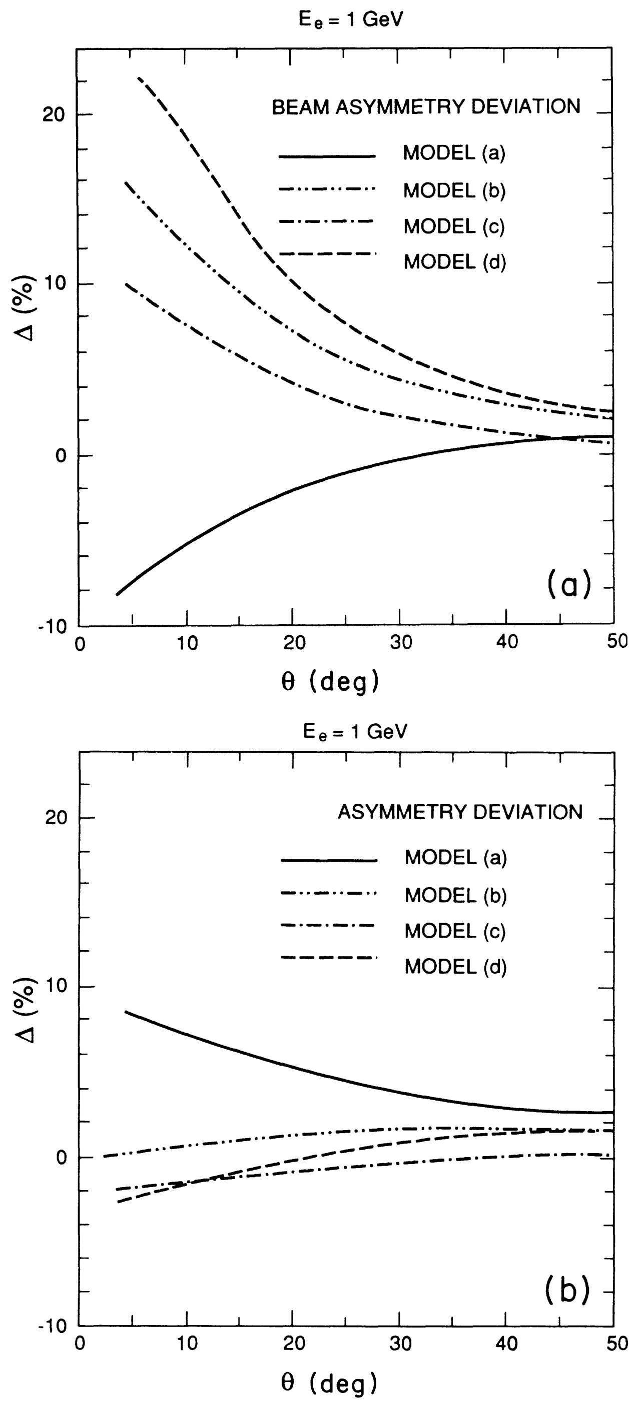

FIG. 5. (a) The beam-asymmetry deviation shown as a function of the electron scattering angle θ_e at $E_e = 1$ GeV for the four different Z'^0 models of Eqs. (11a)–(11d). (b) The target-asymmetry deviation shown as a function of the electron scattering angle θ_e at $E_e = 1$ GeV for the four different Z'^0 models of Eqs. (11a)–(11d).

As mentioned earlier, we adopt $G'/G=\frac{1}{32}$ in making numerical predictions. In the few GeV range, the deviations of the predicted asymmetries from the GSW theory are directly proportional to the value of G'/G, so that predictions for other values of G'/G can easily be deduced. (This proportionality has been checked numerically.)

In Fig. 4(a) we plot the quantity Δ, defined by Eq. (25) for the beam asymmetry, as a function of the electron scattering angle θ_e at $E_e=4$ GeV for the four different Z'^0 models of Eqs. (11a)–(11d), respectively. The behavior at smaller angles is clearly spectacular since it will allow for a clear-cut discrimination among the different models if the asymmetry can be measured to an accuracy of a couple of percent. Our earlier discussion indicates that, as q_λ approaches zero, the deviation of the predicted beam asymmetry from that in the standard GSW theory approaches approximately the constant $[g'_A f'^N_V(0)(G'/G)]/[g_A f^N_V(0)]$. We find, with $G'/G=\frac{1}{32}$ and $q_\lambda \rightarrow 0$,

$$\Delta_A = \begin{cases} -28.9\% & \text{for model (11a)},\\ 57.9\% & \text{for model (11b)},\\ 36.2\% & \text{for model (11c)},\\ 86.8\% & \text{for model (11d)}. \end{cases} \tag{26}$$

The limiting percentage change listed here is very large because of the accidental cancellation that makes $f^N_V(0)$ much smaller than $f'^N_V(0)$. While such a cancellation might have made it easier to discriminate among models, it also makes the experiment more difficult to carry out because of the smallness of the predicted asymmetry.

In Fig. 4(b) we plot the quantity Δ, defined by Eq. (25) for the target asymmetry, as a function of the electron scattering angle θ_e at $E_e=4$ GeV for the four different Z'^0 models of Eqs. (11a)–(11d), respectively. The behaviors at smaller angles are similar to Fig. 4(a), but because of a different accidental cancellation that makes g_V much smaller than g'_V.

The variation from 4 to 1 GeV for the quantity Δ is illustrated by Figs. 5(a) and 5(b), where the quantities Δ defined for the beam and target asymmetries are plotted, respectively, as functions of the electron scattering angle θ_e at $E_e=1$ GeV for the four different Z'^0 models of Eqs. (11a)–(11d). Note that Fig. 5(a) [or 5(b)] is essentially an extrapolation of Fig. 4(a) [or 4(b)] to smaller values of Q^2.

Unless the deviation of the observed asymmetry from the standard GSW electroweak theory is a sizable effect, it will always be useful that a single precision experiment, such as the parity-violation measurement in elastic electron-proton scattering, is combined with other neutral weak interaction experiments, such as neutrino-proton scattering,[16] before an assessment of the presence of the nonstandard Z'^0 boson is made. For instance, a deviation from the standard GSW theory of a couple of percent may also be accounted for by a suitable change in the value of $\sin^2\theta_W$ (without Z'^0). It is, therefore, imperative to carry out different neutral weak-interaction experiments with sufficient precision so that a new physics of some sort, such as that from the Z'^0, will have to be called upon when a universal value of the electroweak mixing parameter $\sin^2\theta_W$ fails to account for the precision data.

IV. SUMMARY

In this paper we have considered the possibility of detecting manifestations of the nonstandard neutral weak boson using a precision measurement of parity violation in elastic electron scattering at an electron beam energy of a few GeV. The numerical results, as shown by Figs. 4 and 5, indicate that, for an assumed Z'^0 mass of about 300 GeV, the deviation of the predicted parity-violating beam and target asymmetries from those given by the standard Glashow-Weinberg-Salam electroweak theory can easily be in the vicinity of several percent. Thus, confirmation of the standard model to within an accuracy of a couple of percent in such measurements should yield a severe constraint on the possible existence of the nonstandard neutral weak boson.

ACKNOWLEDGMENTS

The author wishes to acknowledge the National Science Council of the Republic of China for the support of this work. He also wishes to acknowledge members of the P-2 group at Los Alamos National Laboratory for the hospitality extended to him throughout extended visits, during which part of this work was carried out. He is also grateful to Dr. Hywel White at Los Alamos and Hung-Chi Lin at National Taiwan University for useful conversations.

[1] S. L. Glashow, Nucl. Phys. **22**, 579 (1961); A. Salam, in *Elementary Particle Theory: Relativistic Groups, and Analyticity (Nobel Symposium No. 8)*, edited by N. Svartholm (Almqvist and Wiksell, Stockholm, 1968), p. 367; S. Weinberg, Phys. Rev. Lett. **19**, 1264 (1967); Phys. Rev. D **5**, 1412 (1972).

[2] E. Witten, Nucl. Phys. **B258**, 75 (1985); J. L. Rosner, Comments Nucl. Part. Phys. **15**, 195 (1986); V. S. Kaplunovsky and C. R. Nappi, *ibid.* **16**, 57 (1986); P. Candelas, G. Horowitz, A. Strominger, and E. Witten, Nucl. Phys. **B258**, 46 (1985).

[3] W-Y. P. Hwang, Phys. Rev. D **36**, 261 (1987).

[4] W-Y. P. Hwang (unpublished).

[5] For notation in metric and γ matrices, see, e.g., T. D. Lee, *Particle Physics and Introduction to Field Theory* (Harwood Academic, Chur, Switzerland, 1981).

[6] L. S. Durkin and P. Langacker, Phys. Lett. **166B**, 436 (1986); J. Ellis, K. Enqvist, D. V. Nanopoulos, and F. Zwirner, Nucl. Phys. **B276**, 14 (1986).

[7]V. Barger, N. G. Deshpande, and K. Whisnant, Phys. Rev. Lett. **36**, 137 (1986); Phys. Rev. D **35**, 1005 (1987).

[8]W. J. Marciano and A. Sirlin, Phys. Rev. D **35**, 1672 (1987).

[9]H. Primakoff, in *Muon Physics,* edited by V. W. Hughes and C. S. Wu (Academic, New York, 1975), Vol. II, p. 3.

[10]Particle Data Group, M. Aguilar-Benitez *et al.*, Phys. Lett. **170B**, 1 (1986).

[11]S. Weinberg, Phys. Rev. D **5**, 1412 (1972).

[12]W-Y. P. Hwang, Nucl. Phys. **A329**, 463 (1979).

[13]J. Collins *et al.*, Phys. Rev. D **18**, 242 (1981); R. Mohapatra *et al.*, *ibid.* **19**, 2165 (1979); S. Oneda *et al.*, Phys. Lett. **88B**, 343 (1979); L. Wolfenstein, Carnegie-Mellon University Report No. C00-3066-119, 1979 (unpublished).

[14]N. Baker *et al.*, Phys. Rev. D **23**, 2499 (1981); K. Miller *et al.*, *ibid.* **26**, 537 (1982); T. Kitagaki *et al.*, *ibid.* **28**, 436 (1983).

[15]W-Y. P. Hwang and E. M. Henley, Ann. Phys. (N.Y.) **129**, 47 (1980).

[16]L. A. Ahrens *et al.*, Phys. Rev. D **35**, 785 (1987).